

Application of Parallel Imaging to Reduce SAR in CEST Experiments

E. Vinogradov¹, A. K. Grant¹, P. M. Robson¹, I. Hancu², W. T. Dixon², A. D. Sherry^{3,4}, and R. E. Lenkinski¹

¹Department of Radiology, Beth Israel Deaconess Medical Center, Harvard Medical School, Boston, MA, United States, ²GE Global Research, Niskayuna, NY, United States, ³Department of Chemistry, University of Texas at Dallas, Dallas, TX, ⁴Advanced Imaging Research Center, University of Texas Southwestern Medical Center, Dallas, TX, United States

INTRODUCTION: Chemical Exchange Saturation Transfer (CEST) contrast¹ employs saturation of a small exchanging pool and subsequent reduction of the free water signal. Endogenous molecules^{1,2} (DIACEST) or exogenous complexes of paramagnetic complexes^{3,4} (PARACEST) can be used as CEST agents. The CEST mechanism is very sensitive to the agent's environment such as pH, binding, or metabolic state. Observation of the exchange effects via free water signal results in "amplification" allowing detection of molecules in milliMolar (DIACEST) or in microMolar (PARACEST) concentrations. However, successful detection of CEST effects may require application of RF pulses exceeding FDA approved limitations on Specific Absorption Rate (SAR). This problem is especially crucial for PARACEST agents. Typically PARACEST can be detected in lower concentrations than DIACEST, but requires higher RF power to do so. Here we propose to use Parallel Imaging (PI)⁵⁻⁷ to reduce the average SAR in CEST imaging.

Parallel MRI is an accelerated imaging technique that reduces the number of phase encoding steps required for image reconstruction. This reduction is accomplished by making use of redundant spatial encoding information obtained from arrays of surface coils. PI has become a standard part of clinical imaging protocols, primarily for the reduction of acquisition times. In the context of CEST, parallel imaging can be used to manage SAR and modify image contrast in several ways. By reducing the number of phase encoding steps, one can increase the repetition time (TR) of the sequence while maintaining the same total acquisition time. This will lead to reduction of average SAR, if the same pre-saturation RF characteristics are used. In addition, if the SAR deposition limit is kept constant and TR is increased, higher RF intensities can be used, thus possibly leading to higher CEST effects in some of the B₁ limited applications. In addition, parallel imaging can be used in a standard way to reduce the total acquisition time with other parameters fixed. This may assist to improve temporal resolution of CEST protocol, when multiple acquisitions are required, e.g. for better quantification or to monitor dynamic processes. However, PI reconstructions exhibit decreased Signal-to-Noise Ratio (SNR) due to the reduced number of signal averages acquired, according to a \sqrt{N} rule, and an additional penalty, dependent on the specific receiver-array geometry (the g-factor)⁵. Here we demonstrate the preliminary results of the combination of PI with CEST, and verify that that PI acquisition and reconstruction does not alter observed CEST effects.

METHODS: All of the experiments were performed on a 3T GE Signa scanner using an 8 channel phased array head coil.

CEST: The DIACEST phantom consisted of two tubes (one with 5% Dextrose, one with 9% Saline), immersed in a jar filled with water. Gradient Echo Sequence was used for CEST imaging, with 50msec Fermi pulse with nominal B₁ intensity of 138Hz for saturation. Imaging parameters were: FOV=22cm², TE/TR=6.8/200 msec, matrix size 256x256 and slice thickness 10mm. Images with CEST "on" and "off" were acquired by placing the saturation frequency at +2ppm or -2ppm, respectively, relative to water.

PARALLEL IMAGING: Images were acquired with factor two acceleration, under-sampled in the phase-encoded direction along the length of the tubes. Reconstruction used an in-house, iterative conjugate gradient (CG) algorithm. Coil sensitivities were estimated from full FOV component coil images, normalised by the root-sum-of-squares combination.

IMAGE ANALYSIS: Images with CEST "on" and "off" were acquired with standard and PI-accelerated acquisitions. CEST maps were calculated according to the standard formula $(I(\text{off})-I(\text{on}))/I(\text{off})$

RESULTS and DISCUSSION: Fig. 1 displays images acquired using standard and PI acquisitions, as well as CEST maps. As a first step, the purpose was to verify that the PI recon does not alter the CEST effect, and hence, all of the imaging parameters were kept constant. Susceptibility artefacts are visible and are similar in standard and PI acquisitions. The decrease of the Dextrose signal is also equally evident. The average CEST effect was measured in the ROIs placed in the areas free of susceptibility artefacts (See Fig.1). For Dextrose the CEST effect was 6%±1% in standard images and 6%±2% in the PI reconstructed images (see ROI 3 and 4 in Fig.1). The increase in standard deviation is reasonable, given the SNR reduction by $\sqrt{2}$ due to reduced number of phase encodes. Based on the g-factor map (not shown), the additional SNR penalty was not greater than 1.2 throughout the reconstructed images. The observed CEST effect in Saline was identical with standard and PI methods: -0.7±0.8%, i.e. effectively zero, as expected (ROI 1 and 2). Based on these results, with one dimensional accelerations employed here and CEST effects up to 6% it should be possible to use factor of 3-4 accelerations. Hence, it should be possible to decrease average SAR by a factor of 3-4. In the future, using 3D CEST sequence and suitable hardware, it should be possible to obtain accelerations up to 10-fold⁸, and hence, decrease average SAR by the same factor. Alternatively, it should provide the possibility of using higher power pulses, and achieving higher CEST effects, in particular with PARACEST agents.

Finally, it should be noted that the coil sensitivity estimates required for PI may be obtained with standard imaging sequences, which do not add significantly to the RF deposition in the imaging experiment. An iterative CG solver was chosen for its versatility, and general applicability, to variable density, or non-Cartesian k-space data-acquisition trajectories. This is of importance for imaging *in vivo* where coil sensitivity functions may be estimated from the acquired data itself, minimising the potential of artefacts originating from misregistered image- and coil sensitivity-data. Conversely, since PI is used for reduction of SAR rather than acquisition time limitations, coil sensitivity estimates may be obtained with separate, high resolution images, allowing for high quality PI image reconstruction

REFERENCES: 1. Ward K, *et.al. JMR* 2000; **143**:79.; 2. Zhou J, *et.al. PNMNR* 2006;**48**:109; 3. Zhang S, *et.al. JACS* 2001;**123**:1517; 4. Aime S, *et.al. JACS* 2002;**124**:9364; 5. Sodickson DK, *et.al. MRM*, 1997; **38**:591 6. Pruessmann KP, *et.al. MRM*, 1999; **42**:952; 7. Griswold MA, *MRM*, 2002; **47**:1202 8. Ohliger MA, *et.al. MRM* 2003; **50**:1018.

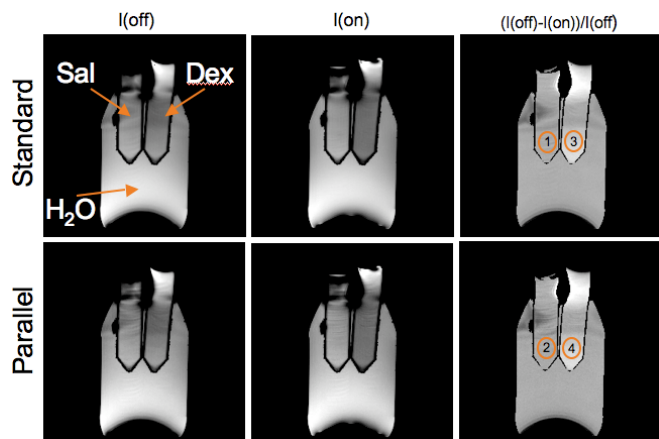


Figure 1. Phantom images acquired using Standard (top) and Parallel (bottom) imaging techniques. Images shown are: CEST off (left), CEST on (middle) and CEST map (right) with ROI placement (see text for more details)